AJNR

Anatomy and Frequency of Large Pontomesencephalic Veins on 3D CT Angiograms of the Circle of Willis

Mehmet Teksam, Sean Casey, Alexander McKinney, Eduard Michel and Charles L. Truwit

Anatomy and Frequency of Large Pontomesencephalic Veins on 3D CT Angiograms of the Circle of Willis

Mehmet Teksam, Sean Casey, Alexander McKinney, Eduard Michel, and Charles L. Truwit

BACKGROUND AND PURPOSE: **The pontomesencephalic veins (PMVs), especially the anterior PMV, are sometimes large enough that they could potentially affect the interpretation of CT angiograms of the circle of Willis. We investigated the frequency and anatomy of visible PMVs on 3D CT angiograms.**

METHODS: **CT angiograms of 211 consecutive patients who underwent CT angiography for a variety of clinical indications were evaluated retrospectively. Images evaluated by consensus between two neuroradiologists were maximum intensity projection and volume-rendered 3D CT angaiograms.**

RESULTS: **Visible PMVs were present on 3D CT angiograms in 11 (5.2%) of 211 patients. Eight of 11 patients had a visible anterior PMV behind the basilar artery. In four patients, the venous caliber of the anterior PMV was sufficiently large enough to be potentially confused with arterial structures. In one patient, 3D CT angiography revealed a large anterior PMV (~2.6 mm in diameter) in the interpeduncular cistern, which had been mistaken for subarachnoid hemorrhage on a nonenhanced CT scan. Two patients had interpeduncular veins of the anterior PMV draping over the dome of a basilar tip aneurysm. In only one patient was the anterior PMV visible possibly owing to arteriovenous malformation. One patient had visible lateral mesencephalic veins, and four patients had visible transverse pontine veins. In one case, on certain views, the transverse pontine veins appeared to arise from the basilar artery.**

CONCLUSION: **Because of their small size, PMVs were seen only infrequently on 3D CT angiograms, but neuroradiologists should be familiar with the normal variants of large PMVs to avoid diagnostic and anatomic confusion.**

Three-dimensional CT angiography has been more widely used in recent years, with numerous reports of its utility in the detection and evaluation of aneurysms of the circle of Willis (1–4). Because of the acquisition technique, this imaging modality depicts both arterial and venous structures. It is not uncommon to see prominent venous structures about the circle of Willis.

The pontomesencephalic veins (PMVs) consist of the pontine veins, which run along the ventral surface of the pons; the interpeduncular veins, which run along the surface of the cerebral peduncles; and the lateral mesencephalic veins, which are localized in the lateral mesencephalic sulci (5). Occasionally, there may be only a single longitudinal vein, which is called the anterior PMV and which runs in the interpeduncular fossa and on the superior and anterior aspects of the belly of the pons between the basilar artery and the brain parenchyma in or adjacent to the midline (6).

The PMVs, especially the anterior PMV, may sometimes become large enough that they may obscure the arterial structures on CT angiograms. Thus, they could potentially affect the interpretation of CT angiograms of the circle of Willis or surgical planning. We retrospectively investigated the frequency and anatomy of visible PMVs on maximum intensity projection (MIP) and volume-rendered 3D CT angiograms.

Methods

We retrospectively reviewed the CT angiograms of 211 consecutive patients who underwent CT angiography for a variety of clinical indications between September 1997 and November 2000.

Three-dimensional CT angiography was performed with 1-mm collimation on single–detector row and 0.5-mm collimation on multi–detector row helical CT scanners (Somatom Plus
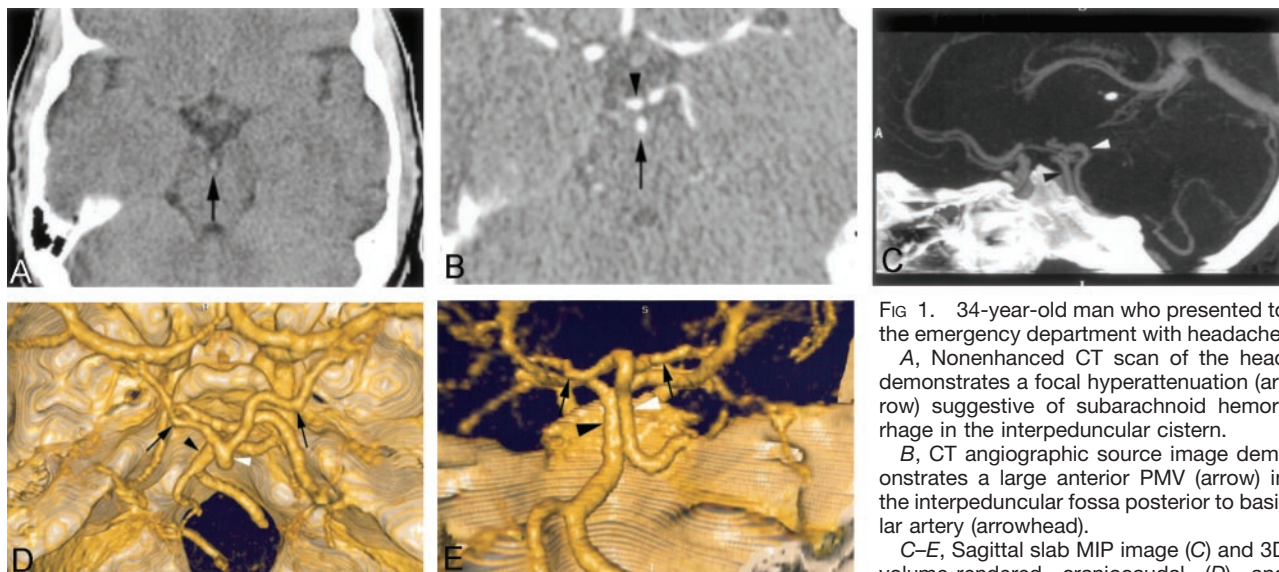
FIG 1.   34-year-old man who presented to the emergency department with headache.

A, Nonenhanced CT scan of the head demonstrates a focal hyperattenuation (arrow) suggestive of subarachnoid hemorrhage in the interpeduncular cistern.

B, CT angiographic source image demonstrates a large anterior PMV (arrow) in the interpeduncular fossa posterior to basilar artery (arrowhead).

C–E, Sagittal slab MIP image (*C*) and 3D volume-rendered craniocaudal (*D*) and posteroanterior (*E*) views demonstrate the large anterior PMV (white arrowhead) posterior to the basilar artery (black arrowhead) and the interpeduncular veins (black arrows). *A* indicates anterior; *P*, posterior; *S*, superior; *I*, inferior.

4 and Somatom Plus Four Volume Zoom CT scanners; Siemens Medical Systems, Forcheim, Germany). Typically, CT angiography was initiated 15–20 seconds after the start of an intravenous infusion of nonionic iodinated contrast material . Contrast material (iohexal [Omnipaque]; Nycomed Ireland Co., Carrigtohill, Ireland) was injected at a rate of 3.3 mL/s for 65 mL and 1.8 mL/s for 35 mL for a total scanning time of 40 seconds on the single–detector row scanner. The injection rate was 5 mL/s for a total scanning time of 15–20 seconds on the multi–detector row CT scanner. The total volume of iodinated contrast material in each study was typically 100 mL. The x-ray tube potential and current were approximately 120 kV and 200 mA, respectively. Table speed for single–detector row and multi–detector row scanners were 1.33–2 mm/s and 2–3 mm/s, respectively. Pitch varied from 1 to 1.5. Scan revolution times of 0.75 second for single–detector row and 0.5 second for multi–detector row scanning were used. Three-dimensional reconstructions were performed on Vital Images Vitrea 2 workstations (Vital Images Inc., Plymouth, MN) by using preset volume-rendered and MIP display algorithms. Notwithstanding the network transfer time of source image data, it took approximately 2–3 seconds to generate the 3D reconstructions on the workstation. Afterward, the neuroradiologist could manipulate the images in a near-infinite number of projections with varying amounts of time needed for review (usually 5–10 minutes). The 3D volume-rendered and MIP images were evaluated by consensus between two neuroradiologists (M.T., S.C.) for conspicuity of PMVs. Although not used to quantitate the frequency of large visible PMVs in this study, source images and multiplanar reformations were also reviewed on the workstation. These images consistently allowed visualization of the typical tiny PMVs that were easily distinguishable from the arteries of the circle of Willis. Such tiny PMVs only resulted in small, incomplete or spotty venous structures on 3D volume-rendered and MIP CT angiographic views.

Results

In 11 (5.2%) of 211 patients, PMVs were visible as venous structures on 3D CT angiograms. Visibility corresponded with a caliber of 0.9 mm or greater, although visibility was somewhat dependent on window level or volume-rendering workstation settings. There was no noticeable difference between size of the venous structures seen on 1.0-mm acquisitions versus 0.5-mm acquisitions. The reviewing neuroradiologists did not notice any difference in identifying prominent venous structures between techniques with a pitch of 1.0 versus a pitch of 1.5 or on the single–detector row versus the multi–detector row scanner.

Eight of 11 patients had a visible anterior PMV behind the basilar artery. In four patients, the caliber of the anterior PMV was sufficiently large to be potentially confused with arterial structures. In these four patients, eight visible interpeduncular veins were detected, which could potentially be confused with the P1 segment of the posterior cerebral artery. One of these patients was a 34-year-old male patient who presented to the emergency department with headache. A nonenhanced CT scan, which was obtained to rule out subarachnoid hemorrhage, appeared to show a small amount of subarachnoid blood layering in the interpeduncular cistern. This pattern was suggestive of a nonaneurysmal perimesencephalic subarachnoid hemorrhage. The CSF analysis from a lumbar puncture was normal, and CT angiography revealed that the attenuation from a large anterior PMV (~2.6 mm in diameter) in the interpeduncular cistern had been mistaken for subarachnoid hemorrhage (Fig 1). The patient had no aneurysm or vascular malformation at CT angiography.

Two of eight patients had interpeduncular veins of the anterior PMV draping over the dome of a basilar tip aneurysm (Fig 2). In only one patient was the anterior PMV visible, possibly owing to a pathologic cause. This patient had an arteriovenous malformation although drainage was not directly into the anterior PMV.

In one of 11 patients, lateral mesencephalic veins were visible. Four of 11 patients had visible transverse pontine veins. In one patient, the transverse pontine vein appeared to arise from the basilar artery and was potentially confused with the anterior inferior cerebellar artery in certain views (Fig 3).

FIG 2.   68-year-old woman with basilar tip aneurysm.

A and *B*, Sagittal slab MIP (*A*) and 3D volume-rendered (Towne's view) (*B*) images demonstrate an anterior PMV (large white arrow in *A*) posterior to the basilar artery (large black arrow in *A*). Note that the interpeduncular veins (small white arrows), which connect the anterior PMV with the basal vein of Rosenthal, are draping over the basilar tip aneurysm (small black arrows). *A* indicates anterior; *P,* posterior; *S,* superior; *I,* inferior.
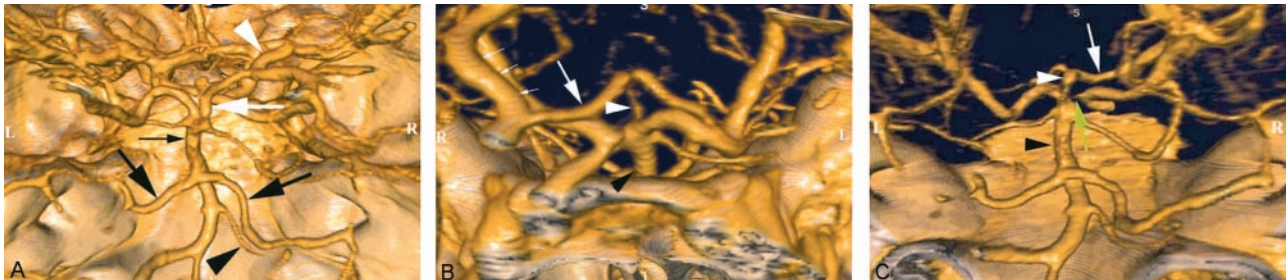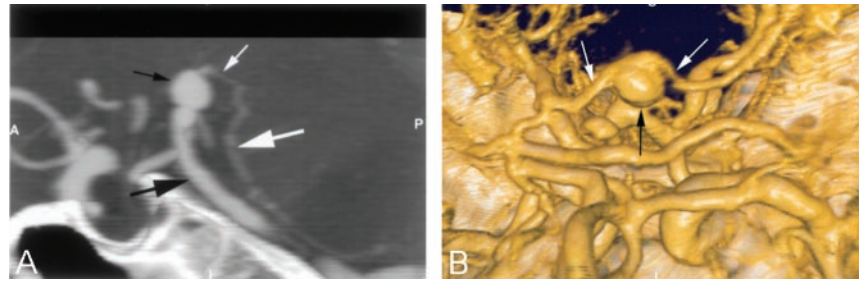

FIG 3.   56-year-old woman evaluated with CT angiography for aneurysm of the supraclinoid segment of the internal carotid artery.

A, Three-dimensional volume-rendered image (posteroanterior view) demonstrates a transverse pontine vein (large black arrows) that appears to be arising from the basilar artery (thin black arrow). This vein could potentially be confused with the anterior inferior cerebellar artery. The actual anterior inferior cerebellar artery is located more inferiorly (black arrowhead). Note that the interpeduncular vein (white arrow), which drains into the basal vein of Rosenthal (white arrowhead), appears to be coming out of the basilar artery.

B and *C,* Three-dimensional volume-rendered images in anteroposterior (*B*) and posteroanterior (*C*) views better demonstrate the anterior PMV (white arrowhead) behind the basilar artery (black arrowhead). Note that the hypoplastic P1 segment of the right posterior cerebral artery (green arrow in *C*) and right interpeduncular vein (large white arrow) draining into the basal vein of Rosenthal (small white arrows in *B*) are now clearly separated. *R* indicates right; *L,* left; *S,* Superior; *I,* inferior.

FIG 4.   *A* and *B*, Anteroposterior (*A*) and lateral (*B*) anatomic diagrams demonstrate the anatomy of the PMVs in relation to the vertebrobasilar system. *1* indicates interpeduncular vein; *2,* basal vein of Rosenthal; *3,* posterior cerebral artery; *4,* superior cerebellar artery; *5,* anterior PMV; *6,* petrosal vein; *7,* anterior inferior cerebellar artery; *8,* vertebral artery; *9,* anterior medullary vein; *10,* posterior inferior cerebellar artery; *11,* basilar artery; *12,* transverse pontine vein; *13,* lateral mesencephalic vein; *14,* internal cerebral vein; *15,* inferior sagittal sinus; *16,* vein of Galen; *17,* sraight sinus; *18,* superior sagittal sinus.
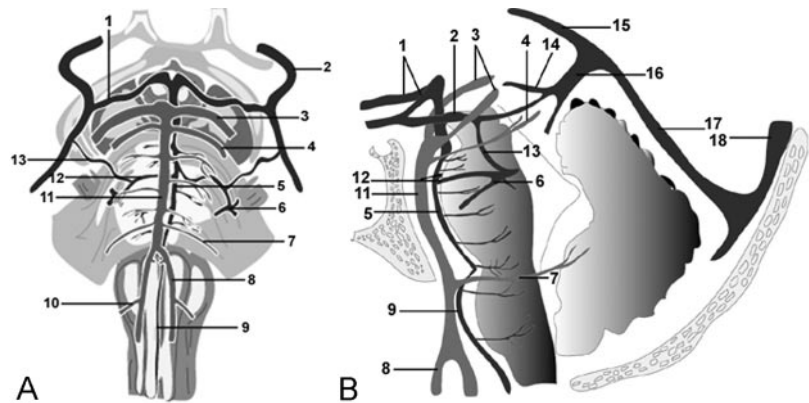
Discussion

During the fourth stage of embryonic development, primitive veins first become identifiable and pass transversely through the pia-arachnoid to reach the dural layer of vessels. Between these primary venous elements, secondary longitudinal anastomoses soon develop on the neural tube and regularly proceed subjacent and at right angles relative to the more developmentally advanced arteries stemming from the midline or nearby. Such longitudinal veins in turn are connected by transverse anastomoses across the midline beneath the basilar artery (5).

The anterior PMV is one of the longitudinal venous channels on the anterior aspect of the brain stem (Fig 4). When it is located in or adjacent to the midline, it is called the median anterior PMV. This median anterior PMV outlines the profile of the depth of the interpeduncular fossa and anterosuperior aspect of the belly of the pons. Sometimes, the anterior PMV runs parasagittally on the anterior aspect of a cerebral peduncle and on the anterolateral aspect of the pons and is then called the lateral anterior PMV. If present, the lateral anterior PMV marks the anterior aspect of a cerebral peduncle and the anterolateral aspect of the pons (5–9). These veins, unlike the arteries, are always strongly adherent to the pons (10). This relation was of great importance to neuroradiologists before the advent of cross-sectional brain imaging. This was because these veins traced the silhouette of the pons and the mesencephalon on conventional angiograms and could, thus, be used to indirectly detect intrinsic brain stem lesions (11, 12). In recent times, the brain stem venous anatomy has been of little interest to radiologists. How-

ever, if these veins are large enough, they may rarely cause some diagnostic difficulties on cross-sectional images. One of our patients had a large anterior PMV, which was confused with subarachnoid hemorrhage because of its location in the interpeduncular cistern, the typical location of nonaneurysmal perimesencephalic hemorrhage (anterior to the brain stem) (13). In this patient, CT angiography helped us to differentiate the large anterior PMV as the cause of hyperattenuation in the interpeduncular cistern (Fig 1), and the patient did not need to undergo any further diagnostic tests.

Awareness of venous anatomy is also important in the interpretation of CT angiograms. With the increasing use of CT angiography of the circle of Willis, radiologists will need to become more familiar with the anatomy of the PMVs. This is because on CT angiograms, unlike MR angiograms on which a saturation band renders the veins invisible, the veins are generally opacified at an attenuation close to that of the arteries. We found these veins to be equally conspicuous with our single–detector row and four channel multi–detector row scanners. We did not evaluate whether protocol alterations designed to generate a more rapid scanning time and higher pitch would decrease visualization of prominent veins. It is plausible that, in the near future, faster scanning techniques using recently introduced 16 channel multi–detector row scanners or future generations of CT scanners may allow the data acquisition to be confined entirely to the arterial phase of the contrast material injection. This would be expected to facilitate interpretation since PMVs would no longer be simultaneously visible with the arteries of the circle of Willis. The PMVs when large may obscure arterial anatomy and lesions and could potentially be confused with normal or variant arterial anatomy, such as a rare variant of duplication of the basilar artery (14) or a persistent trigeminal artery. As in two patients in our series, interpeduncular veins may drape over a basilar tip aneurysm. These veins need to be distinguished from large perforating arteries off the basilar tip as this could affect surgical planning (Fig 2).

The lateral PMV is located on the lateral aspect of the cerebral peduncles, extending inferiorly to join the petrosal vein. The exact location of the lateral PMV varies in some individuals on the anterolateral aspect and in others on the posterolateral aspect of the cerebral peduncles (8). In the past, this vein was sometimes confused on lateral angiographic views with the more posteriorly located anastomotic lateral mesencephalic vein or the more medially located median or lateral anterior PMV.

The lateral mesencephalic vein is located in the lateral mesencephalic sulcus and is a constant tributary of the basal vein of Rosenthal, the PMV, or the petrosal vein (Fig 4) (5, 6, 8, 15).

The anterior medullary vein is a longitudinal venous channel, continuous with the pontine segment of the anterior PMV (Fig 4). Inferiorly, it is continuous with the anterior spinal vein (5, 8).

Transverse pontine veins are often multiple and located at variable levels (superior, middle, and inferior

transverse pontine veins). These transverse pontine veins run laterally to join the petrosal vein, usually at the anterior angle of the cerebellum (Fig 4). In some cases, they drain into the cavernous sinus, inferior petrosal sinus, or medial part of the superior petrosal sinus (5, 8, 9). We saw four visible transverse pontine veins in our review of the CT angiograms of the 211 patients in our series. In one case, the transverse pontine vein appeared to arise from the basilar artery and was potentially confused with the anterior inferior cerebellar artery (Fig 3). Knowledge of the location and anatomy of the transverse pontine vein may, thus, be very important on CT angiograms because it may sometimes be large enough potentially to be confused with adjacent arteries such as the anterior inferior cerebellar artery.

Conclusion

Because of their small size, PMVs only infrequently appear on 3D CT angiograms (5.2% of patients in our series), but neuroradiologists should be familiar with the normal variants of large PMVs to avoid diagnostic and anatomic confusion. In addition, false-positive nonenhanced CT scans for subarachnoid hemorrhage with a nonaneurysmal perimesencephalic pattern may occur owing to a normal variant of a large anterior PMV in the interpeduncular cistern.

References

1. Villablanca JP, Martin N, Jahan R, et al. Volume-rendered helical computerized tomography angiography in the detection and characterization of intracranial aneurysms. *J Neurosurg* 2000;93:254–264
2. Alberico RA, Patel M, Casey S, Jacobs B, Maguire W, Decker R. **Evaluation of the circle of Willis with three-dimensional CT angiography in patients with suspected intracranial aneurysms.** *AJNR Am J Neuroradiol* 1995;16:1571–1578
3. Young N, Dorsch NW, Kingston RJ, Soo RJ, Robinson A. **Spiral CT scanning in the detection and evaluation of aneurysms of the circle of Willis.** *Surg Neurol* 1998;50:50–60
4. Zouaoui A, Sahel M, Marro B, et al. **Three-dimensional computed tomographic angiography in detection of cerebral aneurysms in acute subarachnoid hemorrhage.** *Neurosurgery* 1997;41:125–130
5. Padget DH. **The cranial venous system in man in reference to development, adult configuration, and relation to the arteries.** *Am J Anat* 1956;98:307–355
6. Bradac GB, Holdorff B, Simon RS. **Aspects of the venous drainage of the pons and the mesencephalon.** *Neuroradiology* 1971;3:102–108
7. Hassler O. **Venous anatomy of human hindbrain: a stereomicroangiographic study of the venous angio-architecture and the venous areas of drainage.** *Arch Neurol* 1967;16:404–409
8. Huang YP, Wolf BS. **Veins of the posterior fossa.** In: Newton TH, Potts DG, eds. *Radiology of the Skull and Brain.* St. Louis, Mo: Mosby; 1974;2155–2219
9. Holdorff B, Bradac GB. **The intraparenchymatous pontomesencephalic veins: a radio-anatomical study.** *Acta Anat* 1974;89:333–344
10. Bradac GB. **The ponto-mesencephalic veins: radio-anatomical study.** *Neuroradiology* 1970;1:52–57
11. Sarwar M, Batnitzky S, Schechter M. **Anterior pontomesencephalic vein and basilar artery in exophytic brainstem glioma.** *Radiology* 1997;124:403–407
12. Peeters FLM. **The vertebral angiogram in patients with tumours in or near the midline.** *Neuroradiology* 1973;5:53–58
13. Rinkel GJ, Wijdicks EF, Vermeulen M, et al. **Nonaneurysmal perimesencephalic subarachnoid hemorrhage: CT and MR patterns that differ from aneurysmal rupture.** *AJNR Am J Neuroradiol* 1991;12:829–834
14. Goldstein JH, Woodcock R, Do HM, Phillips CD, Dion JE. **Complete duplication or extreme fenestration of the basilar artery.** *AJNR Am J Neuroradiol* 1999;20:149–150
15. Wackenheim A, Heldt N, Ben Amor M. **Variations in the drainage of the lateral mesencephalic vein.** *Neuroradiology* 1971;2:154–161